A human MAP kinase interactome

Sourav Bandyopadhyay[1,2], Chih-yuan Chiang[3], Jyoti Srivastava[4], Merril Gersten[1,2], Suhaila White[3], Russell Bell[5], Cornelia Kurschner[5], Christopher H Martin[5], Mike Smoot[1], Sudhir Sahasrabudhe[5], Diane L Barber[4], Sumit K Chanda[3,7] & Trey Ideker[1,2,6]

Mitogen-activated protein kinase (MAPK) pathways form the backbone of signal transduction in the mammalian cell. Here we applied a systematic experimental and computational approach to map 2,269 interactions between human MAPK-related proteins and other cellular machinery and to assemble these data into functional modules. Multiple lines of evidence including conservation with yeast supported a core network of 641 interactions. Using small interfering RNA knockdowns, we observed that approximately one-third of MAPK-interacting proteins modulated MAPK-mediated signaling. We uncovered the Na-H exchanger NHE1 as a potential MAPK scaffold, found links between HSP90 chaperones and MAPK pathways and identified MUC12 as the human analog to the yeast signaling mucin Msb2. This study makes available a large resource of MAPK interactions and clone libraries, and it illustrates a methodology for probing signaling networks based on functional refinement of experimentally derived protein-interaction maps.

The mitogen-activated protein kinase (MAPK) pathways are a collection of protein signaling cascades stimulated by a wide variety of extracellular signals, including growth factors, cytokines and environmental stresses[1,2]. Upon activation, MAPK pathways regulate many fundamental cellular functions, including differentiation, proliferation and apoptosis, through the activation of specific transcription factors and other regulatory proteins[3]. Because of this central role in signal transduction, MAPK proteins have been repeatedly implicated in the pathogenesis of cancer and autoimmune diseases, leading to their selection as targets for drug development[4]. MAPK pathways are also well conserved over the eukaryotic kingdom from yeast to man, enabling study of their structure and kinetics through genetic analysis of model organisms[2].

The canonical MAPK pathway consists of three sequentially activated MAPK family members: a MAPK kinase kinase (MAP3K), which activates a MAPK kinase (MAP2K), which in turn activates a MAP kinase (MAPK). It is clear, however, that this canonical pathway is embedded in a rich network of interactions

with a wide variety of other components, including membrane receptors, transcription factors and kinase scaffolds, and that it exhibits extensive cross-talk with other activators and inhibitors of signaling[5]. It has been suggested that a systems-level approach will ultimately be necessary to map these additional components and to understand their MAPK-related functions[3,6].

Toward this goal, we pursued a combined experimental and computational approach to assemble a large resource of MAPK protein interactions and to illustrate methods to functionally explore such a network. This work involved four steps: (i) a screen for physical interactions between MAPK proteins and the rest of the proteome, (ii) an assessment of network quality and functional assessment of MAPK interactors through small interfering RNA (siRNA) screening, (iii) an analysis of the MAPK network to identify potential kinase scaffolds, illustrating how the network can be used as a resource to guide the discovery of new protein functions, and (iv) the identification of interaction modules and the use of evolutionary conservation to aid in functional interpretation of the network. We found evidence that the Na-H exchanger NHE1 functions as a kinase scaffold, and we identified a conserved signaling cascade mediated by the signaling mucin MUC12.

RESULTS

Characterization of a MAPK interactome

We assembled a human MAPK network comprised of protein interactions identified through a two-stage yeast two-hybrid (Y2H) screen. We performed a primary Y2H screen using 86 MAPK-related bait proteins (**Supplementary Fig. 1**) selected by literature curation (Online Methods). Included in these baits were 46 kinases (of which 27 were known MAP-family kinases), 14 transcription factors downstream of MAPK signals and four proteins associated with membrane receptors (**Table 1**). This effort yielded 1,496 protein-protein interactions among 1,096 proteins. As follow-up to this primary screen, we examined 21 secondary baits detected as preys in the first stage (based on their availability as bait cDNA clones). In this round we identified an additional 786 interactions, for a total of 2,269 unique interactions among

Table 1 | Breakdown of network proteins and protein interactions by functional category

	Proteins			Interactions						
	Original Y2H baits	Entire MAPK network	Enrichment P value[a]	MAPK	Other kinases	Transcription factors	Membrane	Cytoskeleton	RNA processing	Other
MAPK	27	29	NA	2	13	22	9	58	21	188
Other kinases	19	65	10^{-9}		15	37	23	76	22	236
Transcription factors	14	89	10^{-7}			36	19	86	26	262
Membrane	4	50	10^{-6}				4	24	20	119
Cytoskeleton	0	193	10^{-32}					47	19	227
RNA processing	0	118	10^{-18}						0	74
Other	22	924	NA							585
Total[b]	86	1,468		313	422	488	218	537	182	1,691

[a]Enrichment P value is based on the probability of identifying an equal or greater number of proteins in the same category at random, assessed via the hypergeometric test with a background of 30,000 genes. NA, not applicable. [b]Total indicates the number of proteins or interactions for a given category.

1,468 proteins (termed the MAPK Y2H network; **Supplementary Table 1**). Bait and prey cDNA clones are available upon request.

Analysis of the MAPK Y2H network revealed 313 interactions involving MAP-family kinases and 422 involving other kinases. After removing the original baits, the MAPK Y2H network was enriched for protein families known to be critical to MAPK signaling, such as membrane proteins and transcription factors (**Table 1**). The network was also highly enriched for proteins involved in RNA binding and processing and in cytoskeletal organization, the latter suggesting the active regulation of microtubule dynamics by MAP kinases or the use of the cytoskeleton as an organizational scaffold in MAPK signaling. It has been postulated that up to one-third of MAP-family kinases are associated with the microtubule cytoskeleton[7].

Many members of the MAPK Y2H network identified here had been implicated in previous screens for genes that function in MAPK signaling. We found that the network (with 86 original baits removed) was highly enriched for proteins that are phosphorylated in response to stimulation of HeLa cells with epidermal growth factor[8] (EGF; 429 of 2,089 phosphorylated proteins; $P < 10^{-170}$). We also found substantial overlap with a screen for kinase activation in fly: the MAPK Y2H network contained 734 genes with *Drosophila* sp. homologs, 92 of which had been shown to be required for the activation of extracellular signal–regulated kinases (ERK) in an unbiased RNA interference screen[9] ($P < 10^{-13}$).

Assessment of MAPK network quality and function

To estimate the sensitivity of the interaction screen (the percentage of true interactions recovered), we assembled a 'positive reference set' of interactions through curation of published literature. This set contained 1,453 previously reported interactions among proteins covered by the MAPK Y2H network (Online Methods). Of the interactions in the positive reference set, we recovered 93 in our MAPK Y2H network, yielding a sensitivity of 6% (**Fig. 1a**). To assess the importance of this number, we next assembled a 'random reference set' of interactions by permutation of the positive reference set to form a non-overlapping set of random interactions, which approximated a set of non-interacting protein pairs[10].

The MAPK Y2H network contained approximately 1% of these randomly chosen interactions, indicating an about sixfold enrichment for the positive reference set over the random reference set.

We could increase sensitivity substantially based on two criteria: (i) observation of an interaction multiple times during the Y2H screen, and (ii) whether the interaction was conserved with yeast. An interaction may be observed multiple times because, during Y2H screening, protein preys are pooled with a particular bait and bait-prey interactions are identified by individual colony selection and sequencing (Online Methods). In our study, we identified many interactions (551 interactions) multiple times through multiple sequenced clones. Similarly, because MAPK pathways are well conserved among eukaryotes[2], evidence that orthologs of the bait and prey can interact in yeast increased the confidence in the interaction. For interactions that were multiply sampled or conserved, respectively, the sensitivity was 19% or 22%, representing a greater than threefold increase in comparison to the entire MAPK Y2H network (**Fig. 1a**). Based on these results, we combined the multiply sampled interactions and conserved interactions to form a 'core MAPK network' of 641 high-confidence interactions (including 47 interactions selected by both criteria; **Supplementary Table 2**). These data have been deposited in the Biological General Repository for Interaction Datasets (BioGRID) database: http://wiki.thebiogrid.org/doku.php/bandyopadhyay2010/.

Evidence for physical interaction may or may not mean that the interaction is functional. Although network function is difficult to assess systematically, classic studies of multiple MAPK pathways have shown that AP-1 or NFκB transcription factors are critical effectors of these pathways under appropriate stimulation[11,12]. We therefore pursued a functional validation strategy based on guilt by association: given MAPK proteins that affect AP-1 or NFκB activation, siRNA knockdown of their functional

Figure 1 | Functional properties of the MAPK network. (**a**) Percentage of positive reference set or random reference set interaction pairs overlapping with each network. Error bars, s.e.m. (**b**) Percentage of MAPK network genes that showed siRNA knockdown of AP-1 or NFκB activity. Random represents the percentage of 45 randomly selected proteins that knock down NFκB levels.
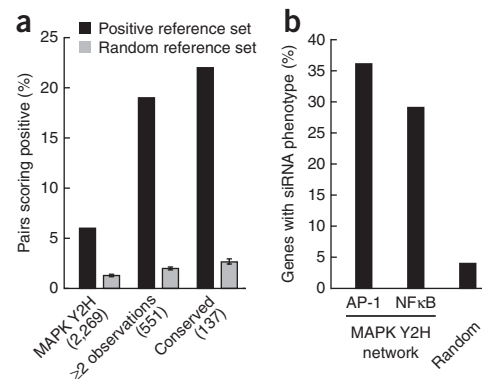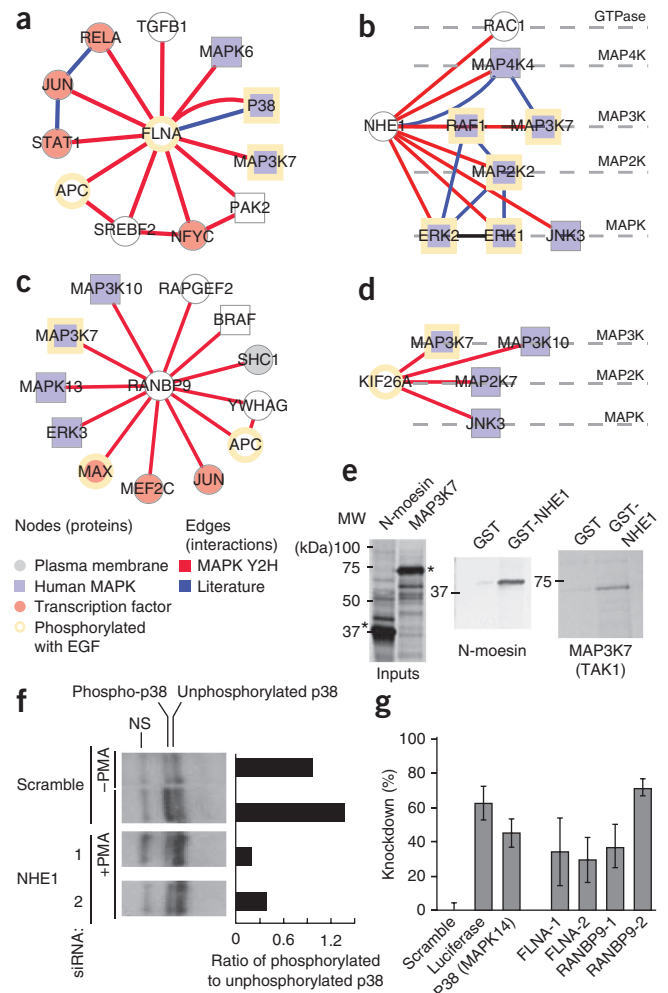
Figure 2 | Protein subnetworks reveal known and putative MAPK scaffolds. (**a**–**d**) Network neighborhoods for filamin protein FLNA (**a**), the Na-H exchanger NHE1 (**b**), RAN binding protein RANBP9 (**c**) and the kinesin family member KIF26A (**d**). Newly identified Y2H interactions (MAPK Y2H) and interactions from literature are shown. Proteins are colored based on their annotation as membrane proteins, MAPKs, as transcription factors or as being phosphorylated with EGF stimulation. Squares indicate kinases. (**e**) Autoradiograms showing binding of *in vitro*–translated MAP3K7 (TAK1) to GST-tagged C terminus of NHE1 or GST alone. N-moesin, a known NHE1 binding partner, was used as a positive control. Expressed input proteins used for *in vitro* binding assays are marked with asterisks. (**f**) Western blot showing phosphorylated (pp38) and total levels of p38, assayed with and without PMA stimulation and two different siRNA knockdowns of NHE1, as indicated. The bars quantify the phospho-p38 to unphosphorylated p38 ratio by image analysis of western blot. As a negative control, PMA stimulation with a scrambled siRNA is shown (scramble, +PMA). A nonspecific band (NS) at a higher molecular weight than p38 is indicated. (**g**) Activity of an AP-1 responsive luciferase reporter by siRNA-mediated knockdown of the indicated genes, upon PMA stimulation. As positive controls, siRNAs targeted to the luciferase reporter and *P38* are shown. Error bars represent s.e.m. with six replicates.

interactors should also modulate these phenotypes. Using this strategy, we selected 14 MAPK-interacting proteins from the MAPK Y2H network that did not have previous evidence for interaction with MAPKs. We systematically knocked down these proteins using four independent siRNAs per gene to mitigate possible off-target effects. We assessed the response to each knockdown by measuring AP-1– or NFκB-mediated transcriptional activation in response to phorbol-12-myristate-13-acetate (PMA) or tumor necrosis factor, respectively. We found that 36% of targeted genes had two or more independent siRNAs that reduced AP-1–mediated transcription (**Fig. 1b** and **Supplementary Fig. 2**). This rate was similarly high (29%) in the case of NFκB. In contrast, siRNAs targeting 45 random genes reduced NFκB-mediated transcription in two cases (4%), almost a tenth the rate for the tested MAPK interactors (**Fig. 1b** and **Supplementary Fig. 2**). This siRNA panel is not a true gold standard; the failure to affect AP-1 or NFκB activity did not negate the corresponding protein-protein interaction, which might be involved in unrelated aspects of MAPK signaling. However, the analysis showed that the 'core MAPK network' recovered ~20% of known interactions among these proteins and that approximately one-third of interactions can be functionally validated using siRNA.

Subnetworks identify NHE1 as a new kinase scaffold

As an example of how the MAPK network can be used to identify new protein functions, we analyzed the network for evidence of MAPK scaffolds. MAPK scaffolds form a signaling apparatus through the simultaneous binding of kinases and their substrates[13]. To identify such scaffolds, we selected interactors of proteins at multiple levels in the MAPK hierarchy for which at least 40% of interactions are with kinases. This selection yielded 10 candidate scaffolds (**Fig. 2a**–**d** and **Supplementary Table 3**). As a positive control, this strategy detected a well-established human MAPK scaffold, the actin-binding protein FLNA, which has been postulated to organize kinase signaling between the membrane and cytoskeleton and to regulate transcription factors such as AP-1 (ref. 14). Of the 11 interactions involving FLNA, seven were with kinases or transcription factors (**Fig. 2a**).

We found that the plasma membrane Na-H exchanger NHE1 interacted with seven MAPK family proteins, spanning all four levels of the MAPK hierarchy including MAP4K4, two MAP3Ks (MAP3K7 and RAF1), MAP2K2 and three MAPKs (ERK1, ERK2 and JNK3) (**Fig. 2b**). NHE1 also interacted with the Rho GTPase Rac1, which can modulate NHE1 activity[15]. In addition to its known role in ion exchange, we postulated that NHE1 may function as a plasma-membrane scaffold for the assembly of signaling complexes[16]. Using tagged NHE1, we confirmed the interaction between the C-terminal cytoplasmic domain of NHE1 and MAP3K7 (TAK1) *in vitro* (**Fig. 2e**). We also identified that two independent siRNAs targeted to the gene encoding NHE1, *SLC9A1* (previously known as *NHE1*) reduced phosphorylation levels of p38 in response to PMA compared to nonspecific scrambled siRNAs, which had no effect, supporting the idea that NHE1 is involved in MAPK pathway function (**Fig. 2f**). Thus, it is possible that the cytoplasmic tail of NHE1 promotes the assembly of a GTPase and MAP-family kinases into (possibly multiple) signaling complexes. Furthermore, as we have previously identified an NHE1 immune complex containing the type II TGF-β receptor, our interaction data suggest that NHE1 may regulate the processing of multiple cell stimuli[17].

We also detected new interactions involving RANBP9, on the basis of which we postulated that it may function as a scaffold in MAP kinase signaling (**Fig. 2c**). Of particular interest is

an interaction between RANBP9 and the RAPGEF2 guanine-exchange factor, which is a member of the Ras subfamily of GTPases. RANBP9 had been originally characterized as binding to the Ras GTPase-binding protein RAN and has been shown to activate the Ras signaling pathway[18]. We found that siRNAs directed to *RANBP9* reduced AP-1–mediated transcription in response to PMA, in a manner similar to knockdown of the known scaffold FLNA (**Fig. 2g**). As controls, scrambled siRNAs had no effect and siRNAs targeting *MapK14* (also known as *P38*),

whose protein product signals upstream of AP-1, reduced AP-1-mediated transcription by 50% (**Fig. 2g**). Although more detailed investigation will be required to validate the role of RANBP9, these results suggest that it may function as a scaffold to organize MAPK signaling upstream of AP-1.

Network modules link MUC12 and HSP90 to MAPK proteins

To shed further light on the structure and function of the core MAPK network (**Fig. 3a**), we analyzed this network to extract conserved and/or species-specific modules (Online Methods). To form these modules, we first combined the core MAPK network with the positive reference set to capture new as well as literature-curated MAPK interactions. We identified network 'modules' as all complete interacting triplets of proteins for which at least two interactions were from the core MAPK network. Triplets and other dense regions of interactions have been shown to be indicative of protein complexes, signaling pathways and other functionally cohesive groups of proteins[19]. In total, we found 134 triplets covering 195 core MAPK Y2H interactions (**Supplementary Table 4**). We next identified a subset of 19 'conserved modules', which were modules for which at least two of the interactions were conserved with yeast. Such modules fell into six connected components, highlighting potential conserved mechanisms of signaling and regulation (**Fig. 3b–g**).

One of these conserved modules included interactions of the MUC12 protein with the MAPK p38 and the Rho GTPase Cdc42 (**Fig. 3b**), suggesting that MUC12 might function in a CDC42-responsive MAPK signaling cascade. We found that multiple distinct siRNA constructs to *MUC12* knocked down both AP-1 activation and p38 phosphorylation in response to PMA (**Fig. 3h,i**), supporting a role for MUC12 in human MAPK signaling. This may occur in analogous fashion to what is seen in yeast, where Cdc42 has been found to interact with the mucin family member Msb2, which functions in kinase signaling[20].

Another conserved module suggested a role for HSP90 members HSP90B1 and HSP90AB1 in the function of MAPK6 (ERK3; **Fig. 3c**), perhaps to stabilize this protein in much the same way as HSP90B1 has been shown to stabilize ERBB2. To investigate this hypothesis, we screened multiple siRNA constructs directed to *HSP90AB1* and *HSP90B1*. We observed a reduction in AP-1–mediated transcription when we targeted *HSP90AB1* and *HSP90B1* (**Fig. 3h**) as
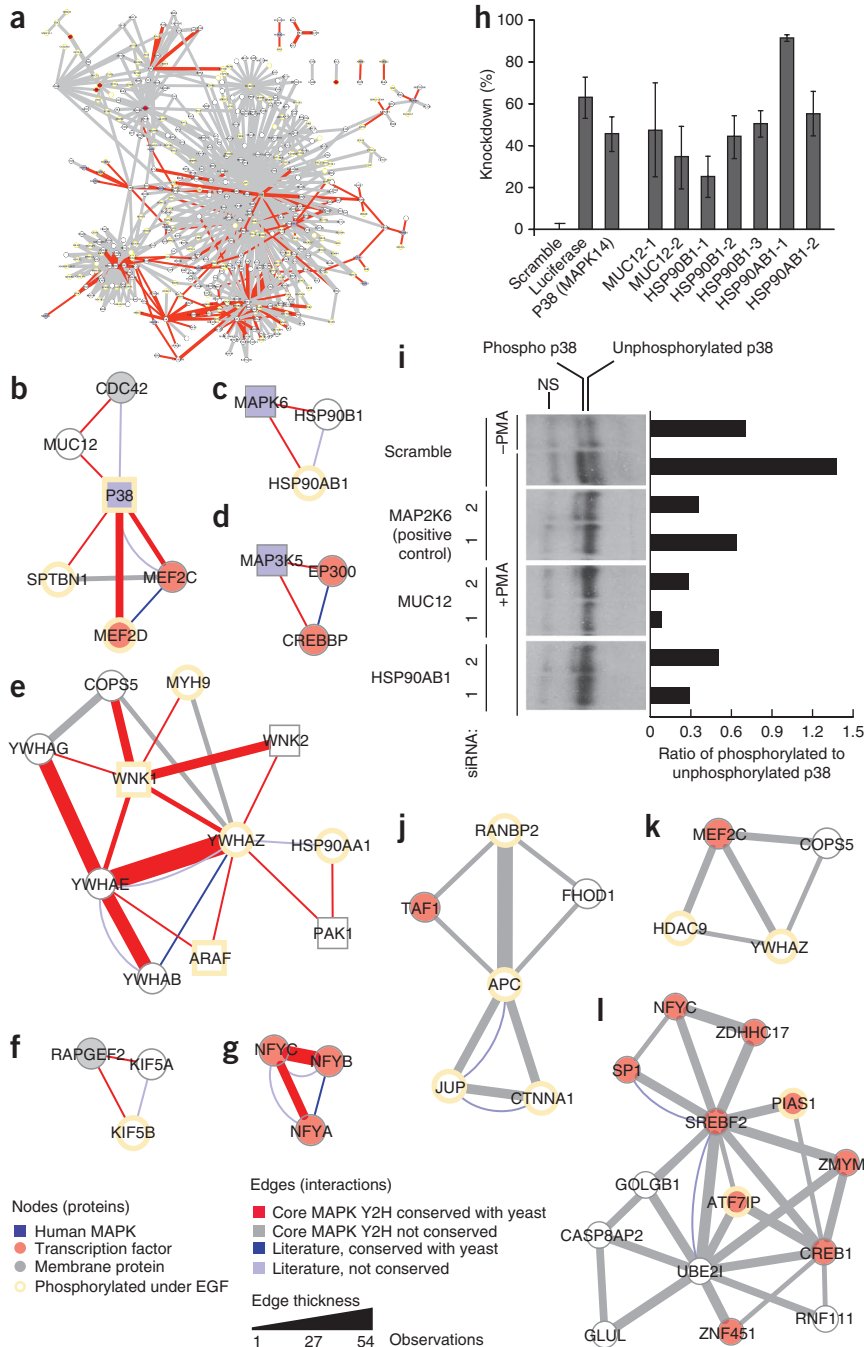

Figure 3 | Functional modules in the core network. (**a**) Bird's eye view of the core MAPK Y2H network. (**b–g**) High-confidence conserved functional modules. (**h**) Activity of an AP-1–responsive luciferase reporter after siRNA transfection targeting members of conserved modules *P38* (*MAPK14*), *MUC12*, *HSP90B1* and *HSP90AB1* (data are presented as in **Fig. 2g**). (**i**) Western blot showing p38 phosphorylation levels after transfection of siRNAs targeting members of conserved modules (as in **Fig. 2f**). (**j–l**) New modules not conserved with yeast.

well as a reduction in phosphorylation levels of p38 when we targeted *HSP90AB1* (**Fig. 3i**), suggesting a role for these HSP90 members in MAPK-mediated signaling.

We also identified three distinct network modules (**Fig. 3j–l**) that were not conserved with yeast. These modules either indicate interactions missing from the current yeast interactome map or machinery that may be present only in higher eukaryotes. One such module provides evidence for an interaction between RANBP2, the GTP-binding protein at the nuclear pore, and the APC tumor suppressor gene, which is known to promote the association of the nuclear pore with microtubules[21]. We also noted a new high-confidence interaction between APC and the catenin CTNNA1 (**Fig. 3j**). As interaction of APC with other β-catenin pathway members has been shown to be critical for WNT signaling, interactions of CTNNA1 with APC may have a role in this pathway as well.

DISCUSSION

Many recently reported studies start with a systematic siRNA screen and then interpret the top hits by projecting them onto a protein interaction network curated from literature[22–24]. Here we reversed this workflow and started with a systematic interactome screen in preparation for targeted siRNA to interpret the high-priority new interactions. This methodology may be particularly useful for the study of cell functions that are not well covered by existing protein interaction maps published in literature. Moreover, such an approach adds functional value to basic interactome mapping efforts, a point that is particularly important given that only a very few previous protein interaction screens have addressed which interactions are functional[25,26].

Beyond the methodological aspects, this work has led to the discovery of more than 2,000 protein interactions related to MAPK signaling, which, along with the associated cDNA clone libraries, constitute a resource for the research community. The quality of the network is comparable to that of previously published Y2H datasets and can be substantially increased by techniques such as multiple sampling and cross-species comparison. We analyzed this network to suggest new kinase scaffolds, demonstrating that, in principle, many discoveries might be mined from these data. Other large-scale technologies such as gene expression profiling, co-affinity purification and phosphoproteomics may add complementary information, yielding a more complete understanding of MAPK signaling in humans and yeast.

METHODS

Methods and any associated references are available in the online version of the paper at http://www.nature.com/naturemethods/.

Note: Supplementary information is available on the Nature Methods website.

AUTHOR CONTRIBUTIONS
S.B., R.B., S.S. and T.I. conceived the study; C.-y.C., J.S., S.W., R.B., C.K. and C.H.M. performed the experiments; S.B., M.G. and M.S. analyzed the data; S.B., T.I., S.S., D.L.B. and S.K.C. wrote the paper and guided the study.

COMPETING FINANCIAL INTERESTS
The authors declare competing financial interests: details accompany the full-text HTML version of the paper at http://www.nature.com/naturemethods/.

Published online at http://www.nature.com/naturemethods/.
Reprints and permissions information is available online at http://npg.nature.com/reprintsandpermissions/.

1. Chang, L. & Karin, M. Mammalian MAP kinase signalling cascades. *Nature* **410**, 37–40 (2001).
2. Widmann, C., Gibson, S., Jarpe, M.B. & Johnson, G.L. Mitogen-activated protein kinase: conservation of a three-kinase module from yeast to human. *Physiol. Rev.* **79**, 143–180 (1999).
3. Kolch, W., Calder, M. & Gilbert, D. When kinases meet mathematics: the systems biology of MAPK signalling. *FEBS Lett.* **579**, 1891–1895 (2005).
4. Johnson, G.L. & Lapadat, R. Mitogen-activated protein kinase pathways mediated by ERK, JNK, and p38 protein kinases. *Science* **298**, 1911–1912 (2002).
5. Kolch, W. Coordinating ERK/MAPK signalling through scaffolds and inhibitors. *Nat. Rev. Mol. Cell Biol.* **6**, 827–837 (2005).
6. Johnson, S.A. & Hunter, T. Kinomics: methods for deciphering the kinome. *Nat. Methods* **2**, 17–25 (2005).
7. Reszka, A.A., Seger, R., Diltz, C.D., Krebs, E.G. & Fischer, E.H. Association of mitogen-activated protein kinase with the microtubule cytoskeleton. *Proc. Natl. Acad. Sci. USA* **92**, 8881–8885 (1995).
8. Olsen, J.V. *et al.* Global, in vivo, and site-specific phosphorylation dynamics in signaling networks. *Cell* **127**, 635–648 (2006).
9. Friedman, A. & Perrimon, N. A functional RNAi screen for regulators of receptor tyrosine kinase and ERK signalling. *Nature* **444**, 230–234 (2006).
10. Venkatesan, K. *et al.* An empirical framework for binary interactome mapping. *Nat. Methods* **6**, 83–90 (2009).
11. Karin, M. The regulation of AP-1 activity by mitogen-activated protein kinases. *J. Biol. Chem.* **270**, 16483–16486 (1995).
12. Rothe, M., Sarma, V., Dixit, V.M. & Goeddel, D.V. TRAF2-mediated activation of NF-kappa B by TNF receptor 2 and CD40. *Science* **269**, 1424–1427 (1995).
13. Whitmarsh, A.J. & Davis, R.J. Structural organization of MAP-kinase signaling modules by scaffold proteins in yeast and mammals. *Trends Biochem. Sci.* **23**, 481–485 (1998).
14. Hayashi, K. & Altman, A. Filamin A is required for T cell activation mediated by protein kinase C-theta. *J. Immunol.* **177**, 1721–1728 (2006).
15. Hooley, R., Yu, C.Y., Symons, M. & Barber, D.L. G alpha 13 stimulates Na+-H+ exchange through distinct Cdc42-dependent and RhoA-dependent pathways. *J. Biol. Chem.* **271**, 6152–6158 (1996).
16. Baumgartner, M., Patel, H. & Barber, D.L. Na(+)/H(+) exchanger NHE1 as plasma membrane scaffold in the assembly of signaling complexes. *Am. J. Physiol. Cell Physiol.* **287**, C844–C850 (2004).
17. Karydis, A., Jimenez-Vidal, M., Denker, S.P. & Barber, D.L. Mislocalized scaffolding by the Na-H exchanger NHE1 dominantly inhibits fibronectin production and TGF-beta activation. *Mol. Biol. Cell* **20**, 2327–2336 (2009).
18. Wang, D., Li, Z., Messing, E.M. & Wu, G. Activation of Ras/Erk pathway by a novel MET-interacting protein RanBPM. *J. Biol. Chem.* **277**, 36216–36222 (2002).
19. Kelley, B.P. *et al.* Conserved pathways within bacteria and yeast as revealed by global protein network alignment. *Proc. Natl. Acad. Sci. USA* **100**, 11394–11399 (2003).
20. Cullen, P.J. *et al.* A signaling mucin at the head of the Cdc42- and MAPK-dependent filamentous growth pathway in yeast. *Genes Dev.* **18**, 1695–1708 (2004).
21. Collin, L., Schlessinger, K. & Hall, A. APC nuclear membrane association and microtubule polarity. *Biol. Cell* **100**, 243–252 (2008).
22. Kim, J. *et al.* Functional genomic screen for modulators of ciliogenesis and cilium length. *Nature* **464**, 1048–1051 (2010).
23. Konig, R. *et al.* Human host factors required for influenza virus replication. *Nature* **463**, 813–817 (2010).
24. Konig, R. *et al.* Global analysis of host-pathogen interactions that regulate early-stage HIV-1 replication. *Cell* **135**, 49–60 (2008).
25. Gunsalus, K.C. *et al.* Predictive models of molecular machines involved in *Caenorhabditis elegans* early embryogenesis. *Nature* **436**, 861–865 (2005).
26. Lunardi, A. *et al.* A genome-scale protein interaction profile of *Drosophila* p53 uncovers additional nodes of the human p53 network. *Proc. Natl. Acad. Sci. USA* **107**, 6322–6327 (2010).

ONLINE METHODS

Data availability. Data are available at http://wiki.thebiogrid.org/doku.php/bandyopadhyay2010/.

Construction of cDNA libraries. Bait and prey cDNAs were cloned as double fusions in plasmids pOBD.111 and pOAD.102 using a previously described Y2H procedure[27]. The cDNAs were cloned between the two-hybrid domain on the 5′ end of the insert and an in-frame selection marker on the 3′ end of the insert. Bait cDNA were cloned between the *GAL4* binding domain sequence and the *TRP1* selectable marker, and prey cDNA were cloned between the *GAL4* transcriptional activation domain and the *URA3* selectable marker. Bait and prey cDNA libraries were prepared by random-primed cDNA synthesis from poly(A)-selected RNA pooled from 22 human tissues (**Supplementary Table 5**) followed by the PCR addition of yeast recombination tails. These cDNAs were then cloned into linearized expression vectors by recombination in yeast. Transformed bait yeast were plated on medium lacking tryptophan to select for in-frame *TRP1* fusions, and prey were selected without uracil for in-frame *URA3* fusions.

Y2H screening. A total of 86 protein baits related to MAPK signaling were selected based on BioCarta (http://www.biocarta.com/pathfiles/h_mapkPathway.asp) and reference 28. Y2H screens were performed in 96-well plates by mating in each well 5×10^6 cells of a yeast clone expressing a single bait with 5×10^6 clonally diverse cells from a prey library. After mating overnight, the well contents were plated on medium that selected simultaneously for successful mating, the expression of the open reading frame selection markers, and the activity of the metabolic reporter genes *ADE2* and *HIS3* (**Supplementary Fig. 3a,b**). Two-hybrid–positive diploids were counted, and up to 48 colonies per mating were picked and transferred to liquid medium (**Supplementary Fig. 3c**). Searches that yielded more than 200 positives were considered to be self-activators (that is, resulting from bait plasmids that activated transcription in the absence of specific protein-protein interactions) and were not analyzed further. Selected colonies were then used as template for separate PCRs to amplify insert sequence from bait and prey plasmids for subsequent sequence determination. Sequence information was processed to prepare the protein-protein interaction dataset. After vector and adaptor clipping, read assembly, repeat masking and contamination filtering, sequences were compared by BLAST (basic local alignment search tool) against RefSeq, and the top hit was used for identification and Entrez Gene mapping. The yeast clones that contained a specific bait-prey interaction pair are available upon request from the authors and can be used to confirm the bait and prey identity, amplify and clone bait or prey inserts, or verify an interaction by another method. All identified interactions have been deposited into the Biological General Repository for Interaction Datasets (BioGRID) database (http://www.thebiogrid.org/). A complimentary Y2H screen for interactions involving human kinases is ongoing at the Max Planck Institute for Molecular Genetics (U. Stelzl, personal communication).

Literature-curated reference sets. To form the positive reference set (PRS), 23,978 literature-curated interactions were obtained from three interaction databases: biomolecular interaction network database (BIND)[29], human protein reference database (HPRD)[30] and BioCarta (http://www.biocarta.com/pathfiles/h_mapkPathway.asp) (**Supplementary Table 6**). To estimate sensitivity for the MAPK Y2H network the PRS was restricted to interactions involving proteins for which at least one interaction was observed in that network dataset (**Fig. 1b**)[10]. To generate a random reference set (RRS), the PRS was randomly permuted, and any overlapping PRS interactions were removed. One hundred such RRS datasets were generated and compared to each network dataset. For each Y2H network, the percentage overlap with the RRS was summarized by its average and s.d. of overlap.

Identification of conserved interactions. For cross-species comparison, the human MAPK Y2H network identified here was supplemented by all protein-protein interactions given in the PRS (see above). A reference network of protein-protein interactions in the yeast *Saccharomyces cerevisiae* was obtained by combining interactions reported in references 31–36. A human protein interaction was considered 'conserved' if both proteins had homologs that interacted in yeast. Sequence homologs between human and yeast were defined using a strict BLAST $E < 10^{-10}$, and to avoid spurious matches owing to large gene families, we allowed no more than ten yeast homologs for each human protein (ten best E values). All conserved interactions are listed in **Supplementary Table 2**.

AP-1 and NFκB luciferase siRNA assay. The HEK293 cell line stably expressed an AP-1 or NFκB responsive promoter fused to a luciferase reporter as previously described[37]. An aliquot of 8×10^3 HEK293 cells was plated into 96-well tissue culture plates, and each well was transfected with 25 ng of indicated siRNA by using Lipofectamine 2000 reagent (Invitrogen). After 72 h of transfection, cells were stimulated with 10 ng ml^{-1} of PMA for 8 h for the case of AP-1 or 10 ng ml^{-1} of tumor necrosis factor (TNF) for 8 h in the case of NFκB. Luciferase activity was measured by using Bright Glow (Promega) according to the manufacturer's instructions. Cell titer was measured by the CellTiter-Glo Luminescent Cell Viability Assay (Promega). Both cell titer and luciferase activity counts were normalized by the median of the scramble siRNAs[38]. All siRNA sequences are listed (**Supplementary Table 7**).

Western blotting for phospho-p38 and *in vitro* binding assays. HeLa cells were transfected using RNAiMAX according to a standard protocol (Invitrogen). After 72 h of transfection, cells were stimulated with 10 ng ml^{-1} of PMA for 8 h. Cells were lysed in buffer containing 25 mM Tris-HCl (pH 7.6), 150 mM NaCl, 1% NP-40, 1% sodium deoxycholate, 0.1% SDS and phosphatase inhibitors (Sigma Aldrich). Ten nanograms of cell lysate was resolved by SDS-PAGE, and blots were immunoblotted with antibodies to the phosphorylated form of p38 (Promega). All blots were developed with horseradish peroxidase (HRP)-conjugated secondary antibodies and ECL reagent (Amersham Biosciences). *In vitro* binding assays for N-terminally GST tagged NHE1 were performed as described previously[39].

27. LaCount, D.J. *et al.* A protein interaction network of the malaria parasite *Plasmodium falciparum*. *Nature* **438**, 103–107 (2005).
28. Qi, M. & Elion, E.A. MAP kinase pathways. *J. Cell Sci.* **118**, 3569–3572 (2005).
29. Bader, G.D. *et al.* BIND–the biomolecular interaction network database. *Nucleic Acids Res.* **29**, 242–245 (2001).

30. Peri, S. *et al.* Development of human protein reference database as an initial platform for approaching systems biology in humans. *Genome Res.* **13**, 2363–2371 (2003).

31. Reguly, T. *et al.* Comprehensive curation and analysis of global interaction networks in *Saccharomyces cerevisiae*. *J. Biol.* **5**, 11 (2006).

32. Ptacek, J. *et al.* Global analysis of protein phosphorylation in yeast. *Nature* **438**, 679–684 (2005).

33. Gavin, A.C. *et al.* Functional organization of the yeast proteome by systematic analysis of protein complexes. *Nature* **415**, 141–147 (2002).

34. Ito, T. *et al.* A comprehensive two-hybrid analysis to explore the yeast protein interactome. *Proc. Natl. Acad. Sci. USA* **98**, 4569–4574 (2001).

35. Ho, Y. *et al.* Systematic identification of protein complexes in *Saccharomyces cerevisiae* by mass spectrometry. *Nature* **415**, 180–183 (2002).

36. Uetz, P. *et al.* A comprehensive analysis of protein-protein interactions in *Saccharomyces cerevisiae*. *Nature* **403**, 623–627 (2000).

37. Chanda, S.K. *et al.* Genome-scale functional profiling of the mammalian AP-1 signaling pathway. *Proc. Natl. Acad. Sci. USA* **100**, 12153–12158 (2003).

38. Konig, R. *et al.* A probability-based approach for the analysis of large-scale RNAi screens. *Nat. Methods* **4**, 847–849 (2007).

39. Denker, S.P., Huang, D.C., Orlowski, J., Furthmayr, H. & Barber, D.L. Direct binding of the Na–H exchanger NHE1 to ERM proteins regulates the cortical cytoskeleton and cell shape independently of H(+) translocation. *Mol. Cell* **6**, 1425–1436 (2000).

doi:10.1038/nmeth.1506